MET.O.14

METEOROLOGICAL OFFICE
BOUNDARY LAYER RESEARCH BRANCH
TURBULENCE & DIFFUSION NOTE

T.D.N. No. 110

A MIXING LENGTH MODEL OF AN ATMOSPHERIC BOUNDARY LAYER - SOME TRIAL INTEGRATIONS

by

C.A.Nash

May 1979

Introduction

A number of straightforward trials with a mixing length model of a horizontally homogeneous boundary layer are presented together with a comparison between this and a second order closure model (Wyngaard et al 1974), in both neutral and unstable situations.

1. The Model

The model iterates to a solution of the Ekman layer equations

$$f(u - u_g) = \partial \tau_y / \partial z$$

$$f(v - v_g) = - \partial \tau_x / \partial z \qquad (1)$$

where $\underline{\tau} = (-\overline{uw}, -\overline{vw}), \quad 0 \leq z \leq D$

We make the mixing length hypothesis

$$\underline{\tau} = \nu \, \partial \underline{u} / \partial z \qquad (2a)$$

where $\nu = l^2 \Delta$ (2b)

$\underline{u}$ is the horizontal velocity, c is a constant (put equal to 0.09 here) and

$$\Delta^2 = \left(\frac{\partial u_i}{\partial x_j} + \frac{\partial u_j}{\partial x_i}\right)^2$$

with the summation convention implied.

l is the mixing length and is given by

$$\frac{1}{l} = \frac{1}{\max(K\phi_m^{-1} z, l_{min}^{(1)})} + \frac{1}{\max(K\phi_m^{-1} z', l_{min}^{(2)})} + \frac{1}{l_0} \qquad z' = z - z_i$$

where z_i is either the height of any inversion present or the penultimate height level in the model. $l_{min}^{(i)}$, l_0 are background mixing lengths which determine l above z_i and in the boundary layer respectively; $\phi_m^{-1} = 1$.

In non-neutral cases, ϕ_m^{-1} has been rather arbitrarily taken to be

$$\phi_m^{-1} = (1 - 5Ri) \quad 0 < Ri < 0.2 \quad ; \quad \phi_m^{-1} = (1 - 20Ri) \quad Ri < 0 \qquad (3^1)$$

where $Ri = \beta \, \partial T / \partial z . \Delta^{-2}$

and β is the buoyancy parameter $(g/\rho)(\partial \rho / \partial T)_p$.

The resolution in the vertical used for the centred difference form of (1) has three or four intervals of differing spacing, adjusted to give a smoothly changing grid length. High resolution is required near the surface and below any inversion present, with the lowest resolution outside the boundary layer. (Cf. Section 2).

Boundary conditions were chosen as

$$\underline{\tau}(z = z_0) = \frac{K^2}{\Psi^2(z_1/z_0, Ri)} (u_1^2 + v_1^2)^{1/2} . (u_1, v_1)$$

$$\partial \underline{u} / \partial z \, (z = D) = 0$$

where $\Psi(z/z_0, Ri)$ is the empirical velocity profile in the surface layer.*

The equations (1) are represented by second-order accurate centred differences with $\underline{u}, \nu$ held on staggered grids. Given $\nu(z)$ the resulting linear equation can be solved directly by matrix inversion to give a new $\underline{u}(z)$ from which an adjusted $\nu(z)$ is deduced by (2). In the neutral case this completes the scheme, but if there is a non-trivial temperature structure this is used to determine Ri which then enters the dynamics through (3). The iteration continues until satisfactory convergence has been achieved.

The temperature is given by the balance equation

$$-\frac{\partial T}{\partial t} = 0 = \frac{T(z) - T_0}{\tau} + \frac{\partial}{\partial z}(\overline{wT}) \qquad (5)$$

within the boundary layer; boundary values of temperature being specified at $z = 0, D$.

Since $\overline{wT}(z=D) = 0$, the first term on the RHS of (5) is neccessary to achieve a steady state when $\overline{wT}(z=z_0) > 0$. This is purely an artifice which also produces a well mixed layer with an inversion above the boundary layer.

To close the equation (5), τ, a characteristic relaxation time, is deduced from the integral form of (5) assuming a simple $T(z)$. T_0 is the linear profile based on the specified temperatures at $z = z_0, D$ and further we assume

$$-\overline{wT} = \nu\, \partial T/\partial z \qquad (6)$$

This completes the formulation in the non-neutral case. However strictly the assumptions are only valid for near neutral conditions.

* i.e. $\dfrac{u}{u_*} = \dfrac{1}{k}\Psi(z/z_0, Ri)$ in the surface layer

$v = 0$

relative to surface stress co-ordinates.

2. Sensitivity trials

The model was integrated for $z_0 = 1\,m$ with various grid spacings to examine the effect on the numerical solution. Table 1 shows the u_* and α_0 obtained for various mean resoutions. The solution does not seem to be very sensitive to the grid chosen

Table 1

Mean resolution at base (m)	Mean resolution in boundary layer (m)	u_*	α_0
33	80	.514	25.0
17	90	.512	25.2
8	90	.511	25.4
2	99	.504	25.3
2	82	.503	25.3
1	82	.506	25.2
.5	99	.504	25.0
.5	83	.503	25.3
.25	100	.503	24.9
Extrapolated ARYA (1974)	.. ..	.47 ± .02	25±2

Using the same parameter values the effect of changing l_0 (equation 3) was inspected. Table 2 shows the results. It is clear that the model is very sensitive to the background mixing length. This is hardly surprising as lo in some measure determines the scale of the turbulence.

Table 2. $z_0 = 1\,m$, $D = 10\,km$. 1m resolution at base and 100m in boundary layer.

Scale length lo	u_*	α_0
25	.414	32.4
50	.454	28.7
100	.505	25.2
100 (D = 3km)	.498	25.7
200	.530	22.1
400	.551	19.9

Figure 1 shows the profiles of $-\overline{uw}$ for some of these trials.

One further test was made varying the amount of smoothing applied to the grid. The effects appeared to be negligable over the range considered in Table 3.

The grid points are first calculated at constant but different spacing within each of up to four intervals covering $(0, D)$ and then adjusted by successively applying a $1-2-1$ smoothing function on the $\{z_i : i = 1, \ldots, N\}$ coordinates of the grid points, i.e.

$$z_1 \rightarrow z_1 \qquad z_i \rightarrow \frac{z_{i-1} + 2z_i + z_{i+1}}{4} \qquad z_N \rightarrow z_N$$

a total of n_{SMTH} times.

Table 3

Model parameters

as Table 2. Scale = 100m

n_{SMTH}	u_*	α_0
30	.505	25.2
45	.506	25.4
60	.506	25.3

3. Model Results

(i) Neutral case.

The resolution was held fixed at 10m near the surface and rising to 130m towards the top of the model at D = 3000m. l_0 was chosen fairly arbitrarily at 100m.

The model was run with differing z_0 so as to give surface Rossby numbers in the range $G/fz_0 = 10^4, 10^{11}$. Fig. 2 shows the variation of u^*/G (G is the geostrophic wind speed) against G/fz_0. The agreement with the empirical curve of Arya (1974) is good but this is not untypical of this type of model. Fig.3 which shows the angle α_0 of the turning of the geostrophic wind from its surface direction is not very good, even though α_0 is difficult to measure reliably.

Fig.4 shows the momentum fluxes compared with the results of Wyngaard's (1974) second-order closure model and a similar model developed by Mason and Sykes (unpublished work). Wyngaard uses methods pioneered by Lumley (1970) for systematic closure of the equations. The comparison is expressed in the scaling of Rossby number similarity theory, and agreement is generally good, although the mixing length models tend to underestimate boundary layer depth. The coordinate system is aligned so that the surface wind is in the x-direction.

Fig.5 considers the dimensionless velocity defects from the models. Agreement is expected outside the surface layer but this is not achieved - the wind tends to geostrophic too rapidly and its magnitude is possibly too great at medium heights.

In all these cases the mixing length result moves closer to that of Wyngaard as $z_0 \rightarrow 0$ but over the range considered this is not considerable.

Clearly the choice of l_0 ,the background mixing length, is quite crucial due to the sensitivity of the model to this parameter. General practice is to let $l_0 = \alpha\delta$ where δ is the boundary layer height and α is a constant. Escudier (1966) has deduced from considering a large number of experiments that $\alpha = .09$; in typical engineering flows α is usually taken about 0.2 . However in our case δ is an unknown parameter.

Blackadar (1962) has suggested that $l_0 = 2.7 \times 10^{-4} G/f$ where G is the geostrophic wind speed or (1965) $l_0 = 6.3 \times 10^{-3} u_*/f$ ($u_*/f \sim \delta$ in a neutral atmospheric boundary layer). (Cf. Blackadar (1975) fo a review).

Thus there is considerable variation in the specification of l_0 and only experiment can provide a firm basis for the choice in a particular case.

unstable case

treatment of mixing length in the surface layer is approximate and te only for near-neutral conditions. However a series of integrations with varying heat fluxes and roughness lengths. The results were ly not sensitive to the grid resolution about the inversion which caps ary layer.

particular an attempt was made to compare directly with the models of (1972) and Wyngaard, but this was unsatisfactory due to differences y they posed their boundary conditions at the inversion.

ypical integration with positive heat flux is now described.

nsider the case $Q_0 = 2.7 \times 10^{-3}$ m °C s^{-1}

$$z_0 = 0.01 \text{ m}$$

$$\delta = 10^3 \text{ m} \quad \text{and} \quad H = 10^4 \text{ m}$$

$$T(D) - T(0) = 1°\text{C}$$

,H are the boundary layer and total height in the model respectively. y state solution is such that

$$u_* = .456 \text{ m s}^{-1}$$

$$z_i = 981 \text{ m} \quad \text{defined as} \quad z_i : -\overline{uw}(z_i) = 0.01\, u_*^2 .$$

$$L = -u_*^3 / k\beta Q_0 = -90 \text{ m}$$

he Monin-Obukov length).

flow, regarded as scaled by Rossby number similarity theory, is rised by the stability parameter

$$z_i / L$$

surface layer. In this case, $z_i/L \approx -11$.

y limited comparison of this solution can be made with Wyngaard's $= -10$ results. Wyngaard has the lid of his model at the inversion all velocity, shear stress and temperature shears to zero there. As a nce the wind is forced to reach its geostrophic value below the inversion t shear across it, in contrast to the model described here where the can be an internal shear layer.

g. 6 shows the profiles of $\underline{u}, T, \nu$ for this solution. The use of (5) is seen to produce an apparently well-mixed boundary layer capped version. The solution is essentially an outer layer solution and is o match a surface layer with its experimentally observed characteristics.

e viscosity increases almost linearly with height near the ground, with $\sim 2ku_*$ compared to ku_* in the surface layer. The viscosity a maximum at about a third the height of the boundary layer and then decays wly in such a way as to maintain an almost constant velocity shear over the depth of the boundary layer: this is almost entirely due to the n of the mixing length scale.

The wind has a marked shear across the inversion cap. This emphasizes the difference between this and the results of Wyngaard and Deardoff.

It is well known that $-\overline{uw}$ tends to a linear function of height as convection becomes dominant, for $-z_i/L$ as low as 10-50, and Fig. 7 shows the results of this calculation are not inconsistent with this.

4. Conclusion

Whilst it has not been possible to check the model fully against the comprehensive models of Deardorff or Wyngaard, it is clear that the qualitative features of the atmospheric boundary layer are captured. The numerical solution is not unacceptably sensitive to changes of grid resolution but the value of background mixing length is clearly very important.

References

Aya, S. P. S. (1975). Geostrophic drag and heat transfer relations for the atmospheric boundary layer, Q.J.R.M.S. 101, 147-161.

Blackadar A.K. (1962) The Vertical Ditribution of Wind and Turbulent Exchange in a Neutral Atmosphere. J.Geophys.Res. 67 3095-3102.

(1965) A single-layer theory of the vertical distribution of wind in a baroclinic atmospheric boundary layer. Final Report AFCRL-65-53-1. Dept. of Met. Penn. State Univ.

Blackadar A.K. (1975) High Resolution Models of the Planetary Boundary Layer. EPA-SRG Ann.Report 1975 Contrib.Penn.State Univ.

Deardorff, J. W. (1972). Numerical Investigation of Neutral and Unstable Planetary Boundary Layers. J.A.S. 29, 91-115.

Escudier M.P. (1966) The Distribution of mixing length in turbulent flows near walls. Imperial College Heat Transfer Scetion. Report TWF/TN/1.

Lumley, J. L. (1970). Toward a turbulent constitutive relation. J.F.M. 41, 413-434.

Wyngaard, J. C., Coté, O. R. and Rao, K. S. (1974). Modelling the Atmospheric Boundary Layer. Advances in Geophysics 18A, 193-212.

E.R.

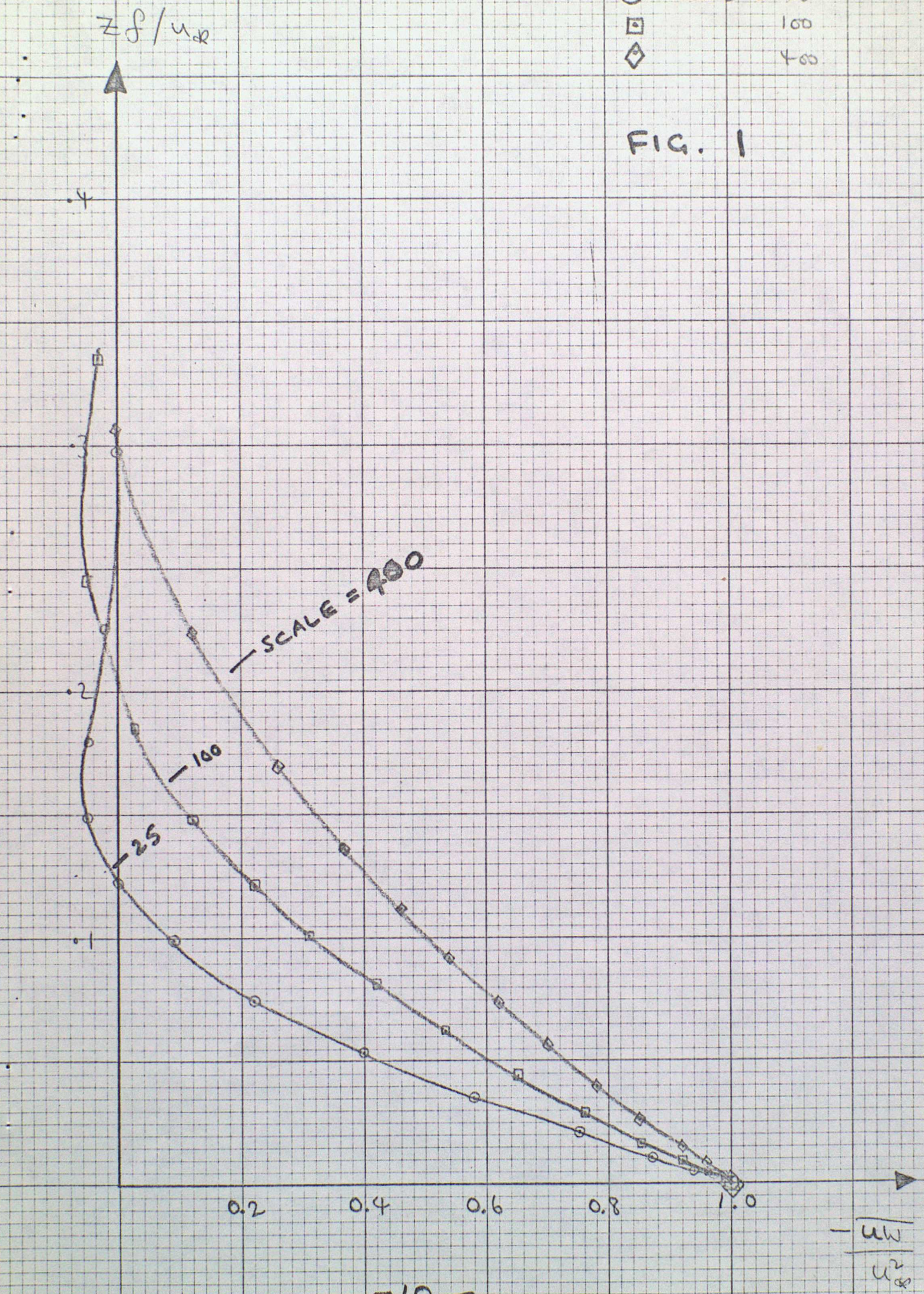

$z f / u_*$
Scale = 25
100
400
SCALE = 400
100
25
.1
.2
.3
.4
0.2
0.4
0.6
0.8
1.0
$-\overline{uw} / u_*^2$

FIG. 1

$\frac{u_*}{G}$, drag coefficient as function of $Ro = \frac{G}{fz_0}$ in neutral conditions.

FIG. 2

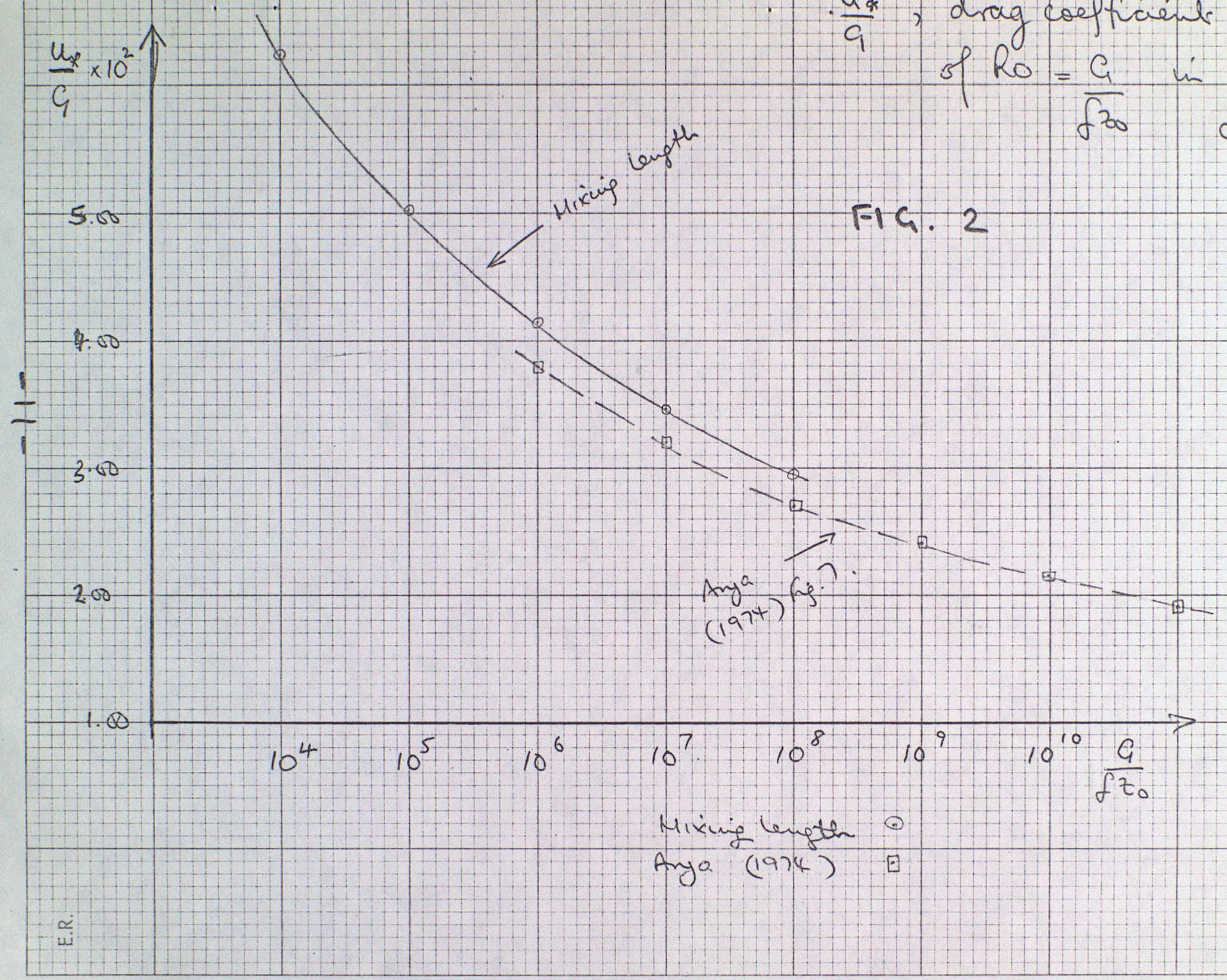

α_0, as function of Ro in neutral conditions

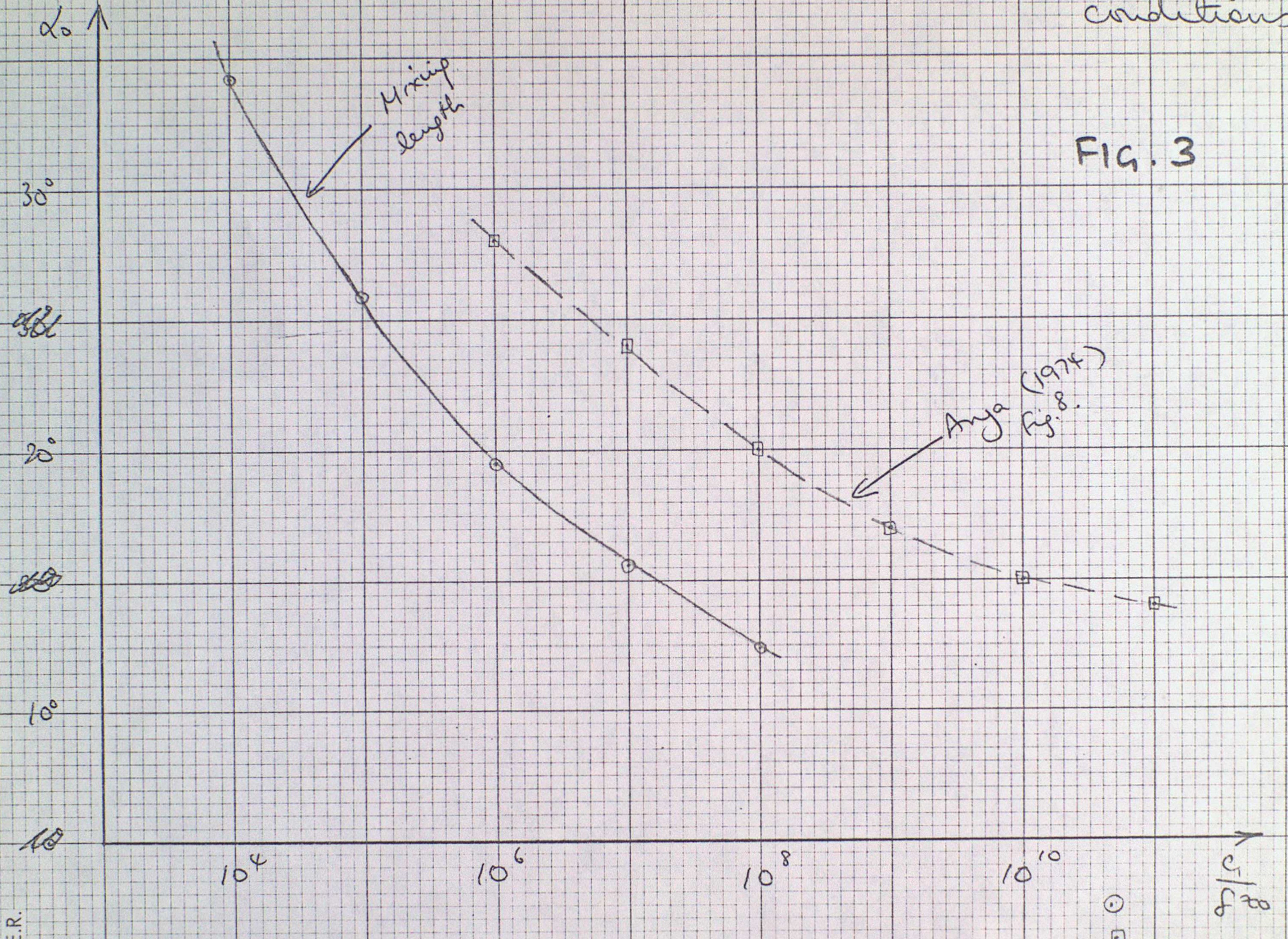

FIG. 3

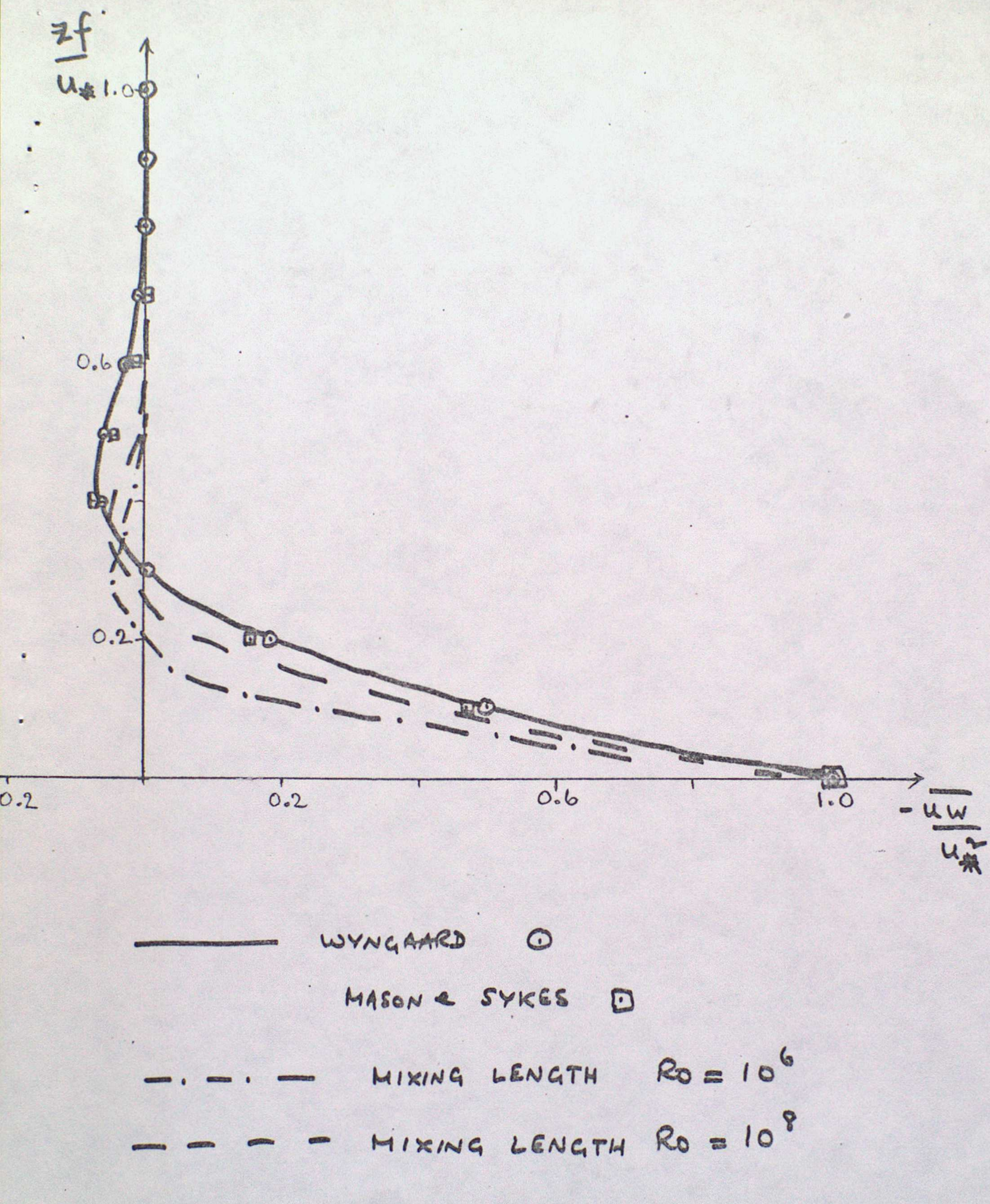

FIG. 4. NEUTRAL MOMENTUM FLUXES.

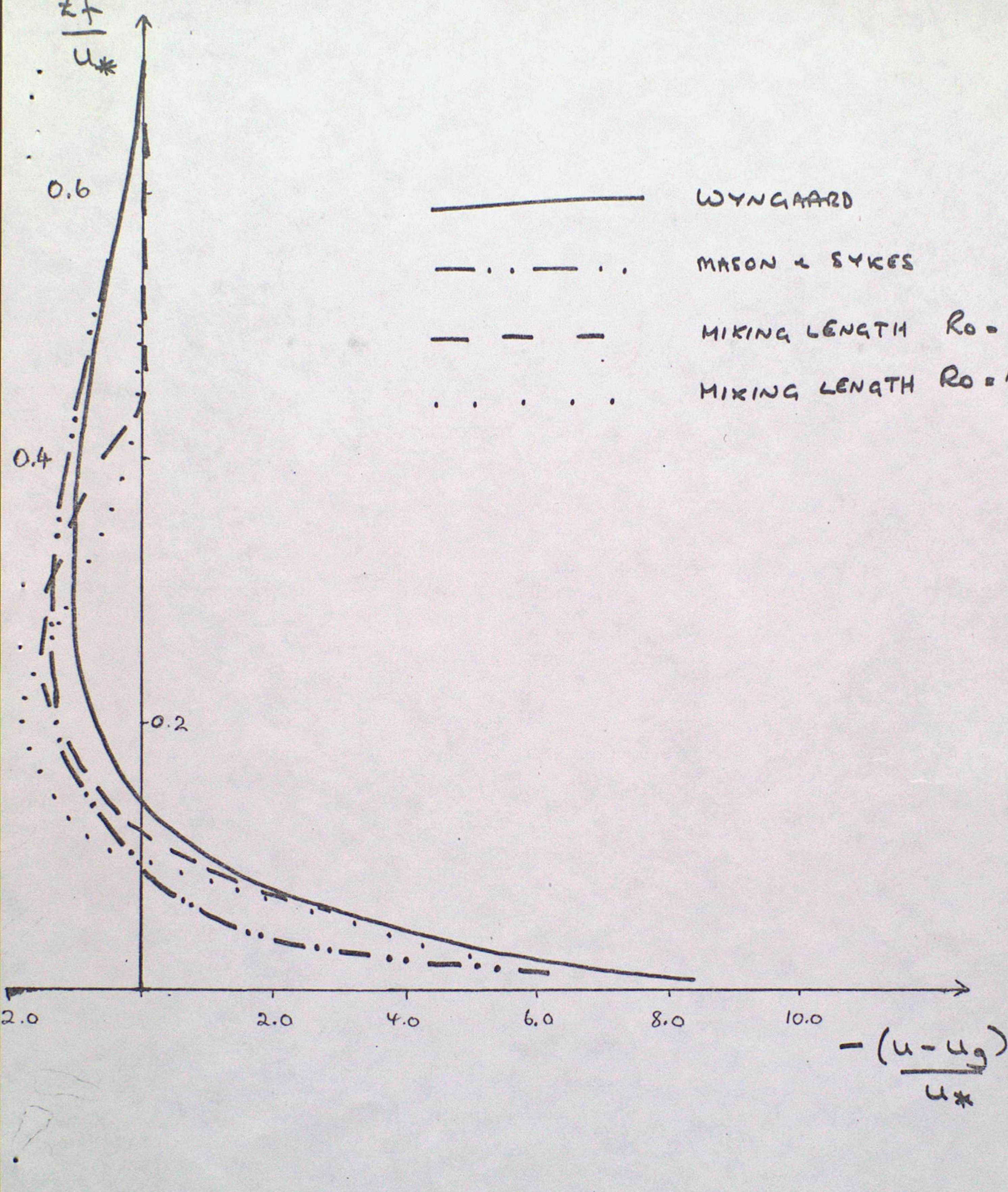

FIG. 5. NEUTRAL VELOCITY DEFECTS.

FIG. 6. PROFILES OF ν, T, $\underline{u}$ FOR UNSTABLE INTEGRATION DESCRIBED IN TEXT.

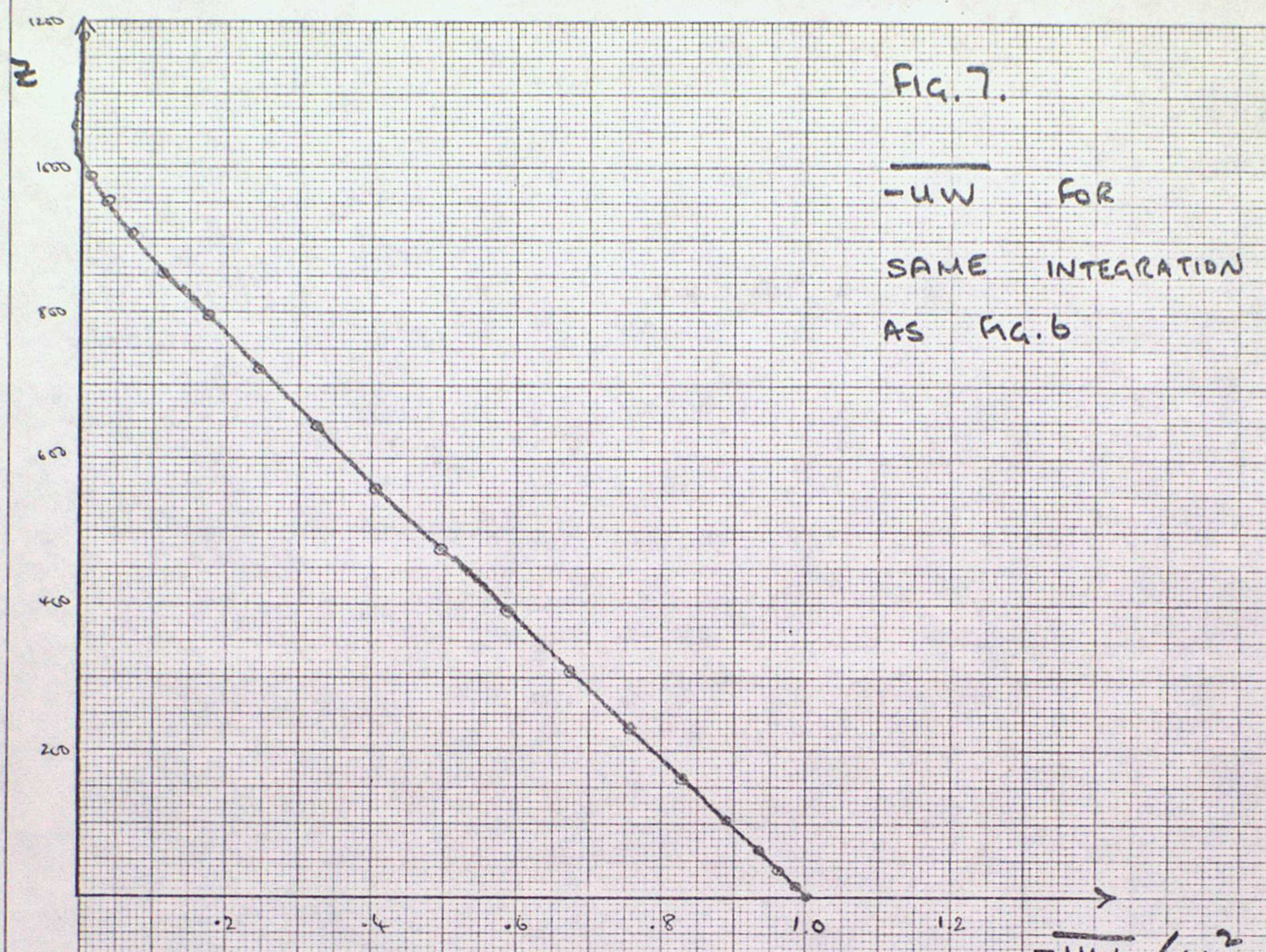

FIG. 7.

$-\overline{uw}$ FOR SAME INTEGRATION AS FIG. 6

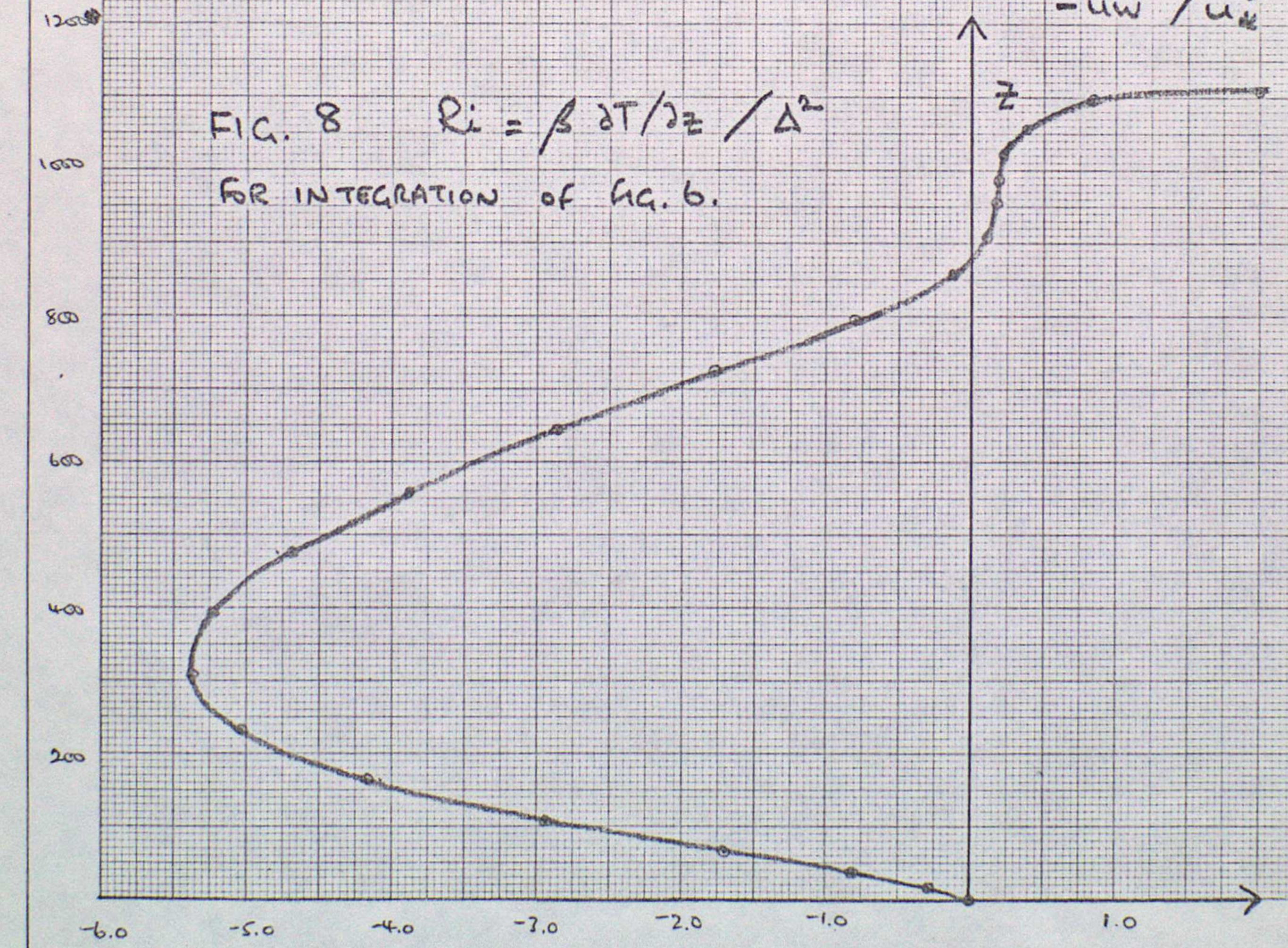

FIG. 8 $Ri = \beta \, \partial T / \partial z \, / \, \Delta^2$

FOR INTEGRATION of FIG. 6.